Available online at www.sciencedirect.com
SCIENCE DIRECT®
Journal of Power Sources 145 (2005) 428–434
JOURNAL OF POWER SOURCES
www.elsevier.com/locate/jpowsour

Design and fabrication of a 100 W anode supported micro-tubular SOFC stack

N.M. Sammes, Y. Du, R. Bove *,[1]

Connecticut Global Fuel Cell Center, University of Connecticut, 44 Weaver Road, Storrs, CT 06269-5233, USA

Accepted 3 January 2005
Available online 25 April 2005

Abstract

Micro-tubular solid oxide fuel cells (SOFC) systems have many desirable characteristics compared to their planar counter-parts, however there are many obstacles and difficulties that must be met to achieve a successful and economically viable manufacturing process and stack design. Anode supported tubes provide an excellent platform for individual cells. They allow for a thin electrolyte layer, which helps to minimize polarization losses, to be applied to the outside of the tube, thus avoiding the difficulty of coating the inside of an electrolyte or cathode supported tubes, or the stack design problem of having a fuel chamber if the anode is on the outside of the tube.

This paper describes the fabrication of supporting anode tubes made of nickel and yttria stabilized zirconia (Ni-YSZ), coated with a thin YSZ electrolyte and a thin coat of lanthanum strontium manganite/cobaltite (LSM) cathode.

The finished tubes were then stacked in an array to provide the specific current/voltage requirements, using a brazing technique. A description of the output characteristics of the single cell, and the characteristics and main issues of a small stack (of 100 W_e designed power output) are also given.

Keywords: Micro-tubular; Anode-support; SOFC-stack; Extrusion

1. Introduction

Solid oxide fuel cells (SOFC) represent an emerging technology for clean, reliable, and flexible power production. The main advantages of power production through SOFCs are due to the high conversion efficiency, the absence of combustion, and the fuel flexibility that allows a variety of fuel (including those derived from renewable sources) to be employed. There is a copious amount of literature describing in detail the advantages and applications of SOFCs [1–7].

The first developed SOFC presented an operating temperature in the range of 900–1000 °C. Siemens-Westinghouse [8] and Rolls Royce [9] are still developing SOFCs to operate in that range of temperature, while a lot of research is now focused in reducing the operating temperature, for solving the sealing and cracking problems, related to SOFC operation [10–13].

There are two main SOFC configurations, i.e. tubular and planar. Planar SOFC performance is theoretically higher than that of tubular, because of the reduced in-plane ohmic resistance. In addition, tape casting and other mass production techniques, for example plasma-spray, can easily be applied for planar SOFC production, thus making possible a substantial production cost reduction. On the other hand, the tubular configuration (TSOFC), because of its geometry, is capable of solving the problems related to cracking, thermo-cycling, start-up time and sealing. Table 1 summarizes the main characteristics of the two configurations.

The selection of suitable materials and the development of specific techniques for TSOFC construction have been described in previous publications by the authors [14–18].

In the present study, a 100 W stack design and construction are presented. The stack is composed of micro-tubular,

* Corresponding author. Tel.: +1 860 4865407; fax: +1 860 4868378.
E-mail address: rbove@engr.uconn.edu (R. Bove).
[1] On leave from Department of Industrial Engineering, University of Perugia, Italy.

0378-7753/$ – see front matter © 2005 Elsevier B.V. All rights reserved.
doi:10.1016/j.jpowsour.2005.01.079

Table 1
Characteristics of tubular and planar SOFC

Characteristics	Tubular	Planar
Power density	Low	High
Volumetric power density	Low	High
High temperature sealing	Not necessary	Required
Start-up cool down	Faster	Slower
Interconnect	Difficult	High cost
Manufacturing cost	High	Low

anode supported SOFCs. Problems related to the performance variation of a single cell, when embedded in a stack, are also identified.

2. Stack configuration

While planar SOFCs are stacked to form a pile of cells, tubular stacks must be assembled in a different configuration. An easy way to arrange single cells is to align them, in order to form a planar multi-cells array (PMA) and then to stack the PMA as if it were a planar cell [19]. The result is that stacks of different sizes can simply be fabricated by assembling different numbers of PMAs. In Fig. 1, a PMA is depicted. As explained in Section 3, the anode represents the internal layer of the tube, while the external surface is the cathode. As a consequence of this configuration, oxidant (air) and fuel can be easily managed and the external leakage is mostly limited to air mass loss. In Fig. 2, a cross section of a PMA is schematically represented. As can be observed, possible leakages are likely to occur from the environment surrounding the tubes (limited by a box) and the external environment. In the configuration of Fig. 2, however, air surrounds the stacked tubes, while fuel flows internally along the tubes, thus the fuel leakage can occur only at the tube extremity. A good brazing between the current collector and the tube, however, is needed to avoid fuel leakage. In Section 4, the tests conducted, and the procedure developed, for brazing the cells to the current collectors are presented.

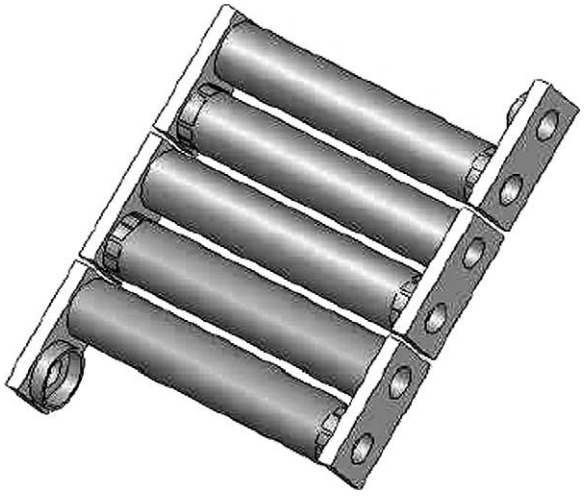

Fig. 1. Planar multi-cells array (PMA).

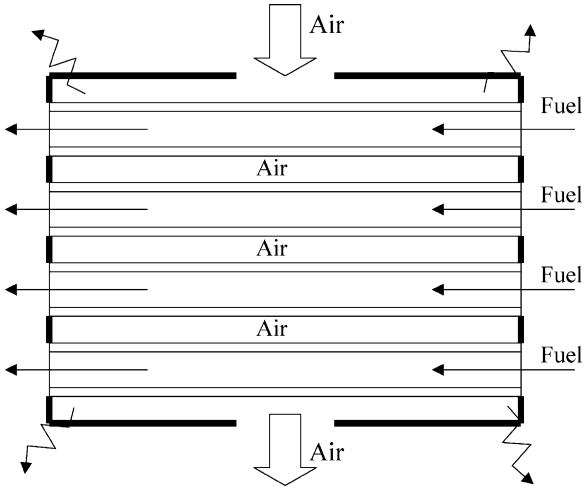

Fig. 2. Schematic cross section of a planar multi-cells array.

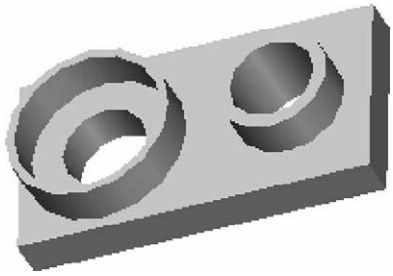

Fig. 3. Current collector.

Fig. 3 depicts the current collector. As can be observed, the two cylinders of the current collector are designed so that one is in contact with the inner part of the cell (i.e. the anode) and the other with the outer (i.e. the cathode), thus every contiguous cell of the PMA is connected in series. Every PMA is then connected in series or parallel, according to the desired current and voltage characteristics.

3. Single cells construction

TSOFC can be externally supported, using a porous media, or can be supported by one of the fuel cell components itself (self-supported) [20]. According to the supporting part, a self-supported FC can be anode, cathode, or electrolyte supported. For the stack construction, based on our previous work [14], an anode supported fuel cell has been selected. The supporting anode tubes are made of nickel and yttria stabilized zirconia (Ni-YSZ), coated with a thin YSZ electrolyte and a thin coat of lanthanum strontium magnate/cobaltite (LSM) cathode [14]. Fig. 4 represents the single cell fabrication process. All the information, relative to tube fabrication procedures, is extensively reported in [14]. After the construction

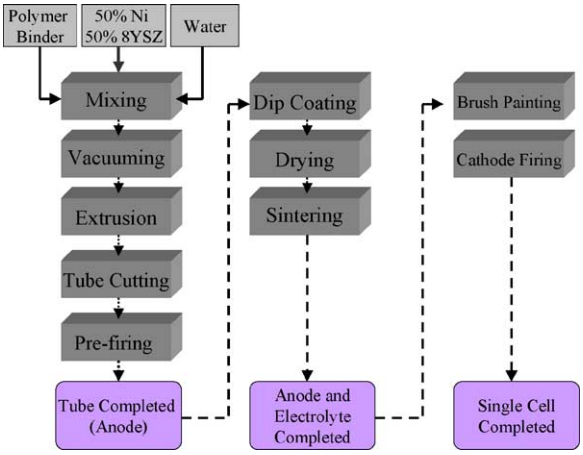

Fig. 4. Single cell production process.

Fig. 5. Picture of the single cells [14].

process is complete, tubes are cut to a length of 110 mm. Fig. 5 is a picture of the single fuel cells [14].

4. Joining current collectors and single cells

Current collectors are joined to the single cells using a brazing technique. An important issue for the joint integrity is the possibility of internal stress, due to the different thermal expansions of the fuel cell components, the brazing material and the current collector. For this reason, materials selection for stacking the cells is crucial. The thermal coefficient of expansion of the tube is estimated to be $12 \times 10^{-6}\,K^{-1}$ [21]. The material selected for the current collector is nickel 200 (Ni 99.5%, Fe 0.15%, CU 0.05%), whose coefficient of thermal expansion is $14 \times 10^{-6}\,K^{-1}$ [22]. The selection of the brazing material is dictated by the need of a compatible coefficient of thermal expansion and a melting point that is lower than that of the tube and the current collector. Pure silver presents a melting point of 961.78 °C and a coefficient of thermal expansion of 18.9×10^{-6} [23], thus it is an ideal candidate as a brazing material.

Silver braze metal in wire form (0.254 mm and 0.762 mm diameter) is placed in the gap between the tube outer diameter (OD) and the cap inner diameter (ID) at the base of the tube, respectively. The interface between the tube OD and the cap ID is designed with enough clearance so that the anode tube and silver wire fits tightly into the nickel end cap. This gap (0.254 mm) makes it possible for the molten silver to flow around and fill the joint volume without overflowing. Lap depth required for brazing is calculated using the following relation [24]:

$$X = \frac{W(D - W)T}{CLD} \tag{1}$$

where W, D, T are the wall thickness, outer diameter and tensile strength of anode tube, respectively. C is the joint integrity factor with a value of 0.8. L is the shear strength of silver braze alloy and X is the lap depth. The brazing process takes place in a furnace, in specific environmental conditions, i.e. in the presence of a slightly reducing/inert atmosphere (98% Ar, 2% H_2) and under the temperature profile of Fig. 6. These conditions are set for avoiding the oxidation of nickel and silver, thereby enhancing the mechanical and the electrical performance of the joint. As seen from Fig. 6, the temperature is ramped up to 800 °C at a rate of 40 °C min^{-1}, and again ramped to 900 °C at 6 °C min^{-1} (to avoid excessive overshoot temperature) and is held at that temperature for approximately 15 min. This provides enough time for the

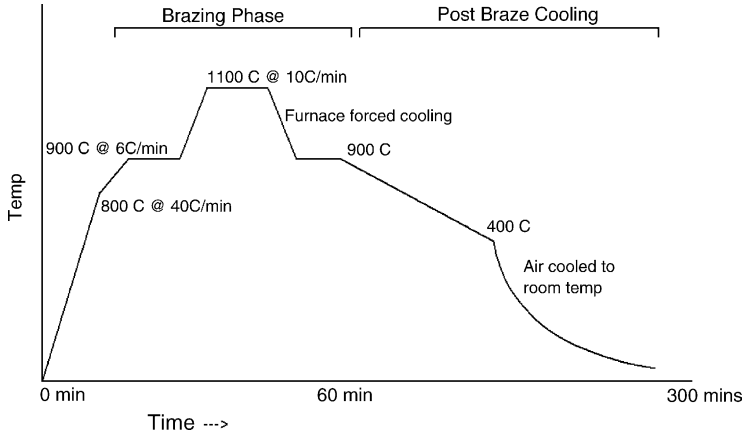

Fig. 6. Brazing temperature profile.

Table 2
Tests results on joint samples

Sample ID	Leakage	Ohmic resistance (milli-ohms)	Torque (kNm)	Micro-structure
1	Yes	Noticeable	0.003	Non-uniform
2	No	4–5	0.0158	Uniform
3	No	4–5	0.0160	Uniform

assembly to come to thermal equilibrium. The temperature is then ramped up at 10 °C min^{-1} to 1100 °C (the brazing temperature), and allowed to soak for 6 min. The assembly is then cooled at 10 °C min^{-1} to 900 °C and allowed to equilibrate for 15 min. It was then cooled at 3 °C min^{-1} to room temperature.

Before assembling the stack, sample joints were realized to perform mechanical, leakage and conductivity tests. Microscopic analysis is also conducted to check the uniformity of the joint. The results of these tests allowed the brazing procedure to be optimized, as described in [24]. Table 2 briefly shows the optimization history. The sample results are reported in the table in chronological order, thus showing the improvements obtained due to each test feedback. As can be seen, the minimum electrical resistance achieved is about 5 mΩ and the nominal failure torque is about 0.016 kNm. The microscopic analysis of the improved joint (sample ID 3 in Table 2) is reported in Fig. 7 [24]. As can be seen, there is very good wetting of both the nickel metal tube and the SOFC anode tube. Silver is observed to diffuse into the ceramic surface as shown in Fig. 7a and b and more distinctively in Fig. 7c. The open porosity of the anode tube helped to facilitate diffusion of silver. From Fig. 7c, it can be seen that the silver has diffused about 50 microns into the ceramic surface.

5. Stack design and expected performance

Before assembling the stack, tests on the single cells are performed. Although SOFC can operate with a variety of fuels, hydrogen is considered in the present study. The tests are conducted in an electric furnace, i.e. under iso-thermal conditions. A constant inlet flowrate of 100 ml min^{-1} is provided to the cell, while current density is varied. First tests are conducted at 850 °C, and then repeated at 800 and 750 °C, respectively. Finally repeated again at 850 °C. Fig. 8 shows the voltage variation during the tests and Fig. 9 the relative

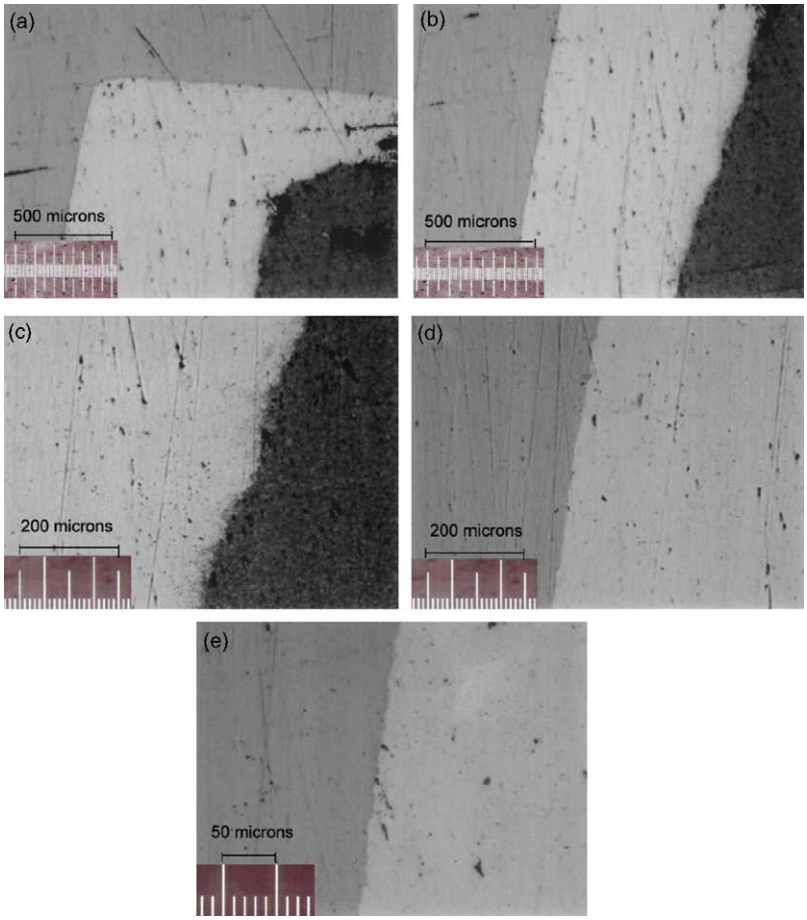

Fig. 7. Optical microscopy of the bond layer; (a) Ni-Ag-YSZ joint corner (b) Ni-Ag-YSZ joint plane (c) Ag-YSZ interface (d) Ni-Ag interface (e) Ni-Ag interface at higher magnification [24].

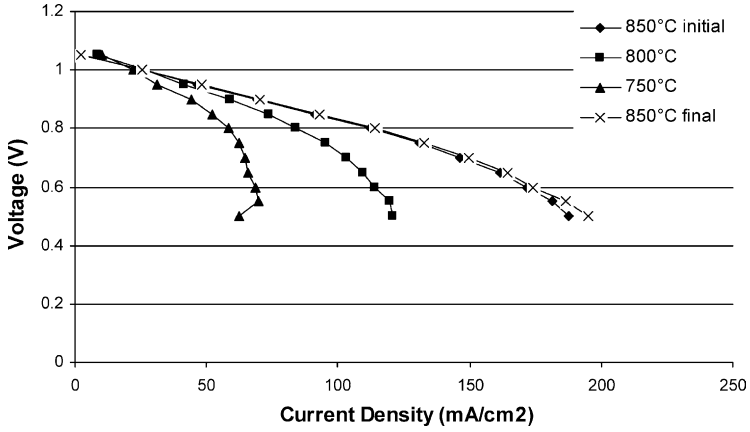

Fig. 8. Voltage–current density tests results at different temperature and constant inlet flow rate.

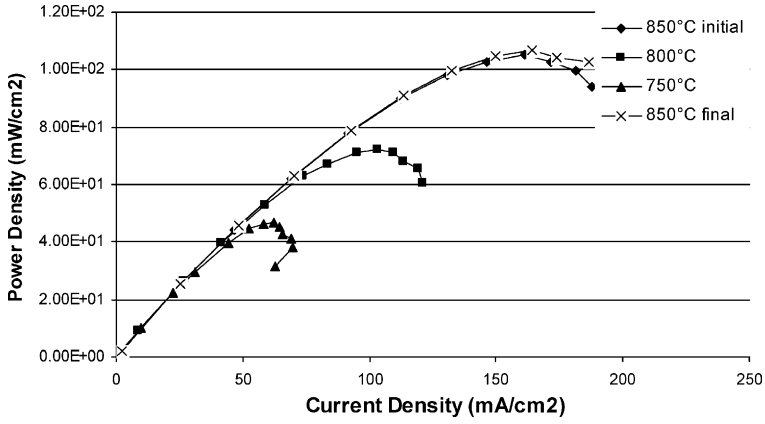

Fig. 9. Power density–current density at different temperature and constant inlet flow rate.

power density. As clearly visible, a change in temperature leads to a remarkable performance variation. This behavior is not surprising, because it is well known that conductivity, as well as the electrode kinetics are connected to the operating temperature. Figs. 8 and 9 also show that temperature cycling does not significantly influence the cell performance. As a results of the tests, the operating temperature, chosen for the stack is 850 °C. The fuel utilization relative to the tests of Figs. 8 and 9 is always below 20%, thus additional tests have been performed, at different flow rates. Flow rates equal to 25, 50, 75 and 100 ml min^{-1}, are provided to the cell and the current density is, for each of them, varied. The fuel utilization is computed as:

$$u_f = \frac{I/(2F)}{n_{\mathrm{H_2,inlet}}} \tag{2}$$

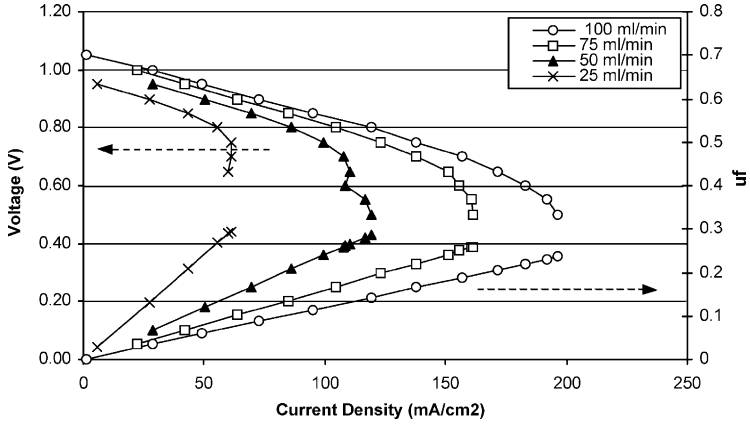

Fig. 10. Voltage variation and relative fuel utilization, for different inlet flow rates.

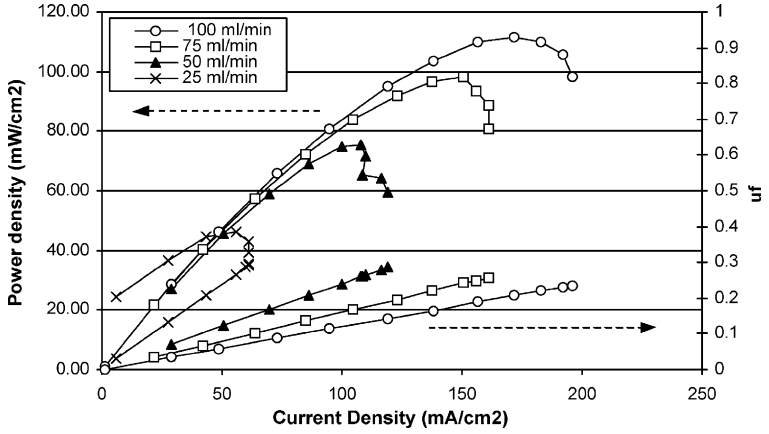

Fig. 11. Power density variation and relative fuel utilization, for different inlet flow rates.

where I is the electric current provided by the cell (express in ampere), F is the Faraday Constant, and $n_{H_2,inlet}$ is the hydrogen molar flow rate provided to the cell.

Fig. 10 represents the result for the voltage, and the relative fuel utilization variation. In Fig. 11, the relative power densities are depicted.

As fully explained in a previous study [25], once the performance of the SOFC is known, the choice of the optimal active surface value (i.e., in the present study, the number of single cells to be stacked) must be determined on an economical basis. If the stack, in fact, operates at high current density a reduction of the investment cost is achieved. However, increasing the current density leads to an efficiency reduction, i.e. an increasing operating cost. The trade-off between operating and investment costs determines the optimal size of the active surface. At the present time, however, SOFCs are still in an experimental phase, and the construction cost is a long way from that expected on the market. For this reason, the number of single cells to be stacked for realizing the stack is chosen on the basis of the maximum performance achieved for the single cells, at reasonable values for the current density and fuel utilization. The design point chosen is characterized by a current density of 119.3 mA cm^{-2}, a voltage of 0.5 V and a power density of 59.5 mW cm^{-2}. The main characteristics of the stack are reported in Table 3. It should be noted that, once in operation, the stack will be tested under different conditions, and the optimal combination of operating parameters that guarantees good performance and stable conditions would be assessed. For this reason, the value of 100 W should not be considered nominal, but a reference condition.

Although the methodology developed for the single cells fabrication and assembly showed promising results and allows the stack to be fabricated, there are still some issues to be considered when passing from single cells to a complete

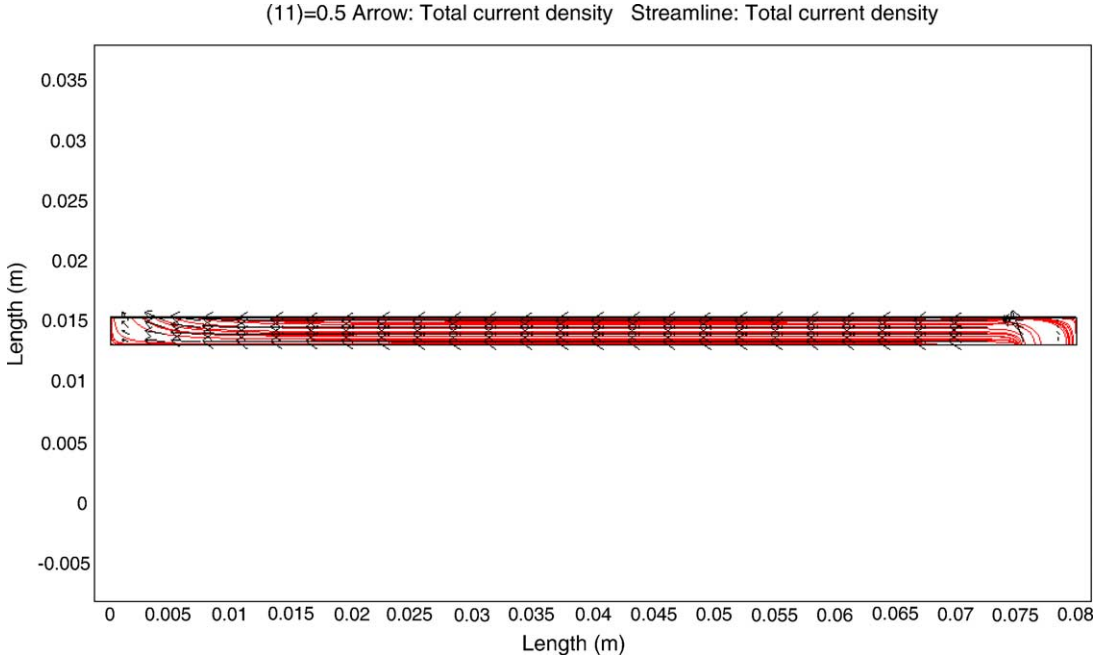

Fig. 12. Cross section of a single cell and relative electrical current path when the voltage between the two electrodes is 0.5 V [19].

Table 3
Main characteristics of the stack at reference condition

Characteristics	
Power (W)	100
Fuel utilization (%)	∼30
Current density (mA cm^{-2})	120
Power density (mW cm^{-2})	59.64
Single cell diameter (cm)	1.32
Single cell length (cm)	11
Electric current (A)	5.44
Number of single cells	40
Stack voltage (V)	20

stack. First, the single cells have been tested in an iso-thermal environment, and, although even the stack can operate under those conditions (i.e. inside a furnace), when a complete system is assembled, an iso-thermal condition does not exist anymore. Secondly, due to the configuration of the current collectors, in-plane ohmic losses can be quite high, thus reducing the overall performance. For a better understanding of this phenomenon, a 2D model of the TSOFC has been implemented and solved using the commercial software FEMLAB®. First results [19] show that the current mostly runs along the cylinder surface, rather than perpendicularly from one electrode to the other, thus causing a relevant performance reduction. Fig. 12 shows the simulated current path together with the velocity distribution of the gas inside the tube. More numerical simulation results on a single cell can be found in another publication by the authors [19], while additional results will be published elsewhere.

6. Conclusions

In the present paper, the work for designing and constructing a 100 W micro-tubular SOFC is illustrated. The realization of the stack is the result of years of interdisciplinary work, focused on single cell construction, brazing technique development, numerical simulations and direct experience of the authors. The stack is composed of 40 single cells, connected, through current collectors, in planar multi-cells array (PMA) configurations. Further tests on the stack will be conducted, thus finding possible stack improvements and optimal operating conditions.

References

[1] J.P. Strakey, M. Williams, W.A. Surdoval, S.C. Singhal, U. S. DOE Solid Oxide Fuel Cell Program, in: Proceedings of Sixth European Solid Oxide Fuel Cell Forum, vol. 1, 48–59, June 28–July 2, 2004, Lucerne, Switzerland, 2004.
[2] G.A. Tompsett, C. Finnerty, K. Kendall, T. Alston, N.M. Sammes, J. Power Sources 86 (2000) 376–382.
[3] S.C. Singhal, Solid State Ionics 135 (2000) 305–313.
[4] M. Doriya, Solid State Ionics 152/153 (2002) 383–392.
[5] H. Tu, U. Stimming, J. Power Sources 127 (2004) 284–293.
[6] EG&G Technical services, Inc. Fuel Cell Handbook, sixth ed., U.S. Department of Energy, November 2002.
[7] J. Larminie, A. Dicks, Fuel Cell Systems Explained, J. Wiley and Sons Ltd., England, 2000.
[8] S. Vora, Small-scale low cost SOFC power system, in: Proceedings of the SECA Annual Workshop and Core Technology, May 11–13, Boston, MA, 2004.
[9] G. Agnew, A. Spangler, Reducing fuel cell system costs without lowering operating temperature, in: Proceedings of the 2nd International Conference on Fuel Cells Science Engineering and Technology, June 14–16, Rochester, NY, 2004.
[10] P. Banace, N.P. Brandon, B. Girvan, P. Holbeche, S. O'Dea, B.C.H. Steele, J. Power Sources 131 (2004) 86–90.
[11] J. Love, R. Ratnaraj, Operation of CFCL's all-ceramic stack technology, in: Proceedings of Sixth European Solid Oxide Fuel Cell Forum, vol. 1, 355–362, June 28–July 2, 2004, Lucerne, Switzerland, 2004.
[12] K. Ogasawara, Y. Baba, K. Fujita, H. Kameda, H. Yakabe, Y. Matsuzaki, T. Sakurai, Development of anode supported planar SOFC with metallic interconnectors operated at reduced temperature, in: Proceedings of Sixth European Solid Oxide Fuel Cell Forum, vol. 1, 394–400, June 28- July 2, Lucerne, Switzerland, 2004.
[13] B. Zhu, J. Power Sources 114 (2003) 1–9.
[14] Y. Du, N.M. Sammes, J. Power Sources 136 (2004) 66–71.
[15] Y. Du, Fabrication and characterization of micro-tubular solid oxide fuel cells, University of Waikato Ph.D. dissertation, 2004.
[16] Y. Du, N.M. Sammes, J. European Ceram. Soc. 21 (6) (2001) 727–735.
[17] Y. Du, N.M. Sammes, G.A. Tompsett, J. European Ceram. Soc. 20 (7) 959–965.
[18] Y. Du, N.M. Sammes, G.A. Tompsett, D. Zhang, J. Swan, M. Bowden, J. Electrochem. Soc. 150 (2003) A74–A78.
[19] R. Bove, N.M. Sammes, P. Lunghi, Design of a tubular SOFC stack aided by numerical simulations, in: Fuel Cell Seminar 2004, November 1–5, 2004, San Antonio, TX, 2004.
[20] N.Q. Minh, T. Takahashi, Science and Technology of ceramic fuel cells, Elsevier, Amsterdam, 1995.
[21] A.V. Durov, B.D. Kostjuk, A.V. Shevchenko, Y.V. Naidich, Mater. Sc. Eng. A290 (2000) 86–189.
[22] W.B. Hanson, K.I. Ironside, S.A. Fernie, Acta Mater. 48 (2000) 4673–4676.
[23] D.R. Lide, CRC Handbook of Chemistry and Physics, 77th ed., CRC Press, N.Y, 1996.
[24] A. Basak, R. England, N.M. Sammes, Determination of the mechanical integrity of ceramic-to-metal braze joints in SOFC interconnect applications, in: Proceedings of Sixth European Solid Oxide Fuel Cell Forum, vol. 2, 950–959, June 28–July 2, 2004, Lucerne, Switzerland, 2004.
[25] R. Bove, N. Sammes, Optimal SOFC size design for minimal cost of electricity achievement, Fuel Cells Sci. Technol., ASME 2 (1) (2005) 9–13.